Proceedings of ICRC 2001: 1848 © Copernicus Gesellschaft 2001

ICRC 2001

Simulation in 3D of electron transport & emissions in radio galaxies

I. L. Tregillis[1], **T. W. Jones**[1], **and D. Ryu**[2]

[1]School of Physics and Astronomy, University of Minnesota, USA
[2]Department of Astronomy and Space Science, Chungnam National University, Korea

Abstract. We have developed numerical techniques to treat CR acceleration at shocks in multidimensional MHD simulations of astrophysical objects. These allow us to study production, transport and emissions produced by CRs inside very complex and unsteady flows. Here we report results of 3D supersonic jet simulations designed to model radio galaxy formation. Initial findings demonstrate several important physical points: (1) The flows, including the jets, are highly unsteady. Clear jet termination shocks are uncommon, so that CRs are accelerated more by a complex web of shocks in the flow "head". (2) The energy spectrum of the accelerated CRs is spatially and temporally complex, and not simply the canonical "strong-shock" power law. (3) Magnetic fields within the "backflow cocoon" are highly intermittent, so conventional "aging" models, based on synchrotron losses are not reliable.

1 Introduction

Radio galaxies illuminate some of the most energetic events in the universe. Giant "lobes" of nonthermal relativistic plasma are apparently inflated by light, hypersonic jets formed as a byproduct of accretion onto massive black holes in the associated galactic nucleus. That nonthermal plasma is directly and dramatically visible through synchrotron and Compton-upscattered emissions and indirectly visible through its influence on the ambient thermal intergalactic plasma. The interactions between the high speed jets and the ambient medium are thought to produce strong shocks within the ambient medium as well as the jet and its "cocoon" of previously deposited jet plasma. Those collisionless shocks should be sites of efficient particle acceleration.

In the radio galaxy cartoon the outflowing plasma jet ends in a strong termination shock usually considered to be the principal location for particle energization. The observed nonthermal radio and X-ray emissions are explained through the transport of relativistic electrons and embedded magnetic fields into the cocoon where those electrons suffer both adiabatic and radiative losses.

The extant literature provides many analytic models for particle acceleration in the posited termination shock (e.g., Heavens & Meisenheimer (1987)) and increasingly sophisticated multi-dimensional HD or MHD numerical simulations of the plasma flows (e.g., Clarke (1996)). However, only very recently has it been possible to include meaningful direct treatments of the particle acceleration and transport in the simulated flows. Our effort, described briefly here, is the first to include this physics in sufficient detail to study time dependent electron acceleration and transport along with synthetic observations of the nonthermal emissions from the simulated objects (Jones et al., 1999; Tregillis et al., 2001). That opens the door for the first time to direct detailed exploration of the relationships between dynamics and emissions.

2 Methods

We have computed three dimensional simulations in which there are a bulk magnetized plasma and a passive population of relativistic "CR" electrons. The bulk flow dynamics is treated with a second-order accurate, conservative "TVD" MHD code (e.g., Ryu et al. (1998)). The relativistic electron distribution function, $f(\boldsymbol{x}, p, t)$ is followed by way of a simplified "diffusion - advection" equation through a scheme described in Jones et al. (1999). In smooth flows the method is based on second-order van Leer spatial advection and a finite volume momentum advection. Away from shocks spatial diffusion is neglected in this implementation. At shocks $f(\boldsymbol{x}, p, t)$ is modified to agree with the conventional test-particle solution for steady diffusive shock acceleration theory, since we consider only electrons with momenta $p/mc < 10^5$, which should be accelerated instantaneously compared to a dynamical time step in the simulations. In some runs fresh relativistic electrons are shock injected at a rate pro-

Correspondence to: T. W. Jones (twj@astro.umn.edu)

portional to that of the bulk plasma flow through the shock. A preexisting relativistic electron population also enters the computational grid in the jet along with the bulk plasma. The electron momentum space is efficiently divided into only a handful of logarithmic bins (typically 8) by modeling $f(p)$ as $f(p) \propto p^{-q(p)}$, where $q(p)$ varies slowly with momentum. We are able to study the evolution of the electron population including effects of adiabatic and radiative losses.

We make synthetic observations of the simulated objects using in each spatial zone approximate, self - consistent emissivities for synchrotron and "inverse-Compton" processes. Those depend on the electron population as well as the magnetic and radiation fields present. Surface brightness maps can be constructed for any viewing orientation by ray tracing (see Tregillis et al. (2001)). Those maps may then be analyzed using standard observing procedures with conventional astronomical image processing software.

3 The Simulations

We are in the process of exploring a wide range of simulated radio galaxy behaviors. Here we outline some of our early findings and illustrate them through images from a sample simulation. The radio galaxies simulated so far are formed by light jets propagating through a uniform ambient medium. Each jet enters with a steady, "top hat" velocity profile surrounded by a thin transition sheath. The core jet speed is Mach 80 with respect to the ambient medium and is set to 0.05c. The inflowing jet is in approximate pressure balance with the ambient medium and has a density contrast, $\rho_j/\rho_a = 10^{-2}$. Thus, internally the jet flow is Mach 8. The jet radius is 2kpc. There is an initially axial ambient magnetic field, B_{x0}, with pressure 1% of the thermal pressure. The inflowing jet carries a helical field set to match the ambient field on the jet axis and boundary. We apply a slow 5^o precession at the jet orifice to break the symmetry, ensuring a truly three-dimensional calculation from the beginning.

We have so-far explored three idealized models for the evolution of the electron spectra. In two of those we consider all the relativistic electrons to enter at the jet base with a simple powerlaw momentum spectrum given by $q = 4.4$, which corresponds to a synchrotron spectral index $\alpha = 0.7$. That spectrum is evolved according to the diffusion-convection equation with appropriate source terms, including the effects of diffusive acceleration at shocks, but no additional electrons are injected at local shocks. We have considered two such cases; one in which radiative losses are turned off to explore the effects of the complex shock structures in these flows. This is our "control model". The other related electron model also turns on synchrotron radiative losses in the embedded magnetic field, in order to explore spectral "aging" of the electrons. The third electron model supplies only a small initial population of electrons from the jet base, since it explores primarily the behaviors of electrons injected at shocks within the flows, as described above.

The simulation shown here is a "control model" run. In this case we have used a nonuniform spatial grid with a finely resolved section along the nominal jet axis and spanning the central $\frac{2}{3}$ of the grid in the transverse directions. The transverse space is then extended with geometrically growing zones. The grid extends a distance along the jet axis equal to 115 jet radii, and 114 jet radii in the other two dimensions. Five zones span a jet radius at the orifice. Previously reported three-dimensional simulations used a uniform grid spanning a smaller volume, but spread 15 zones across a jet radius.

4 Results

We previously reported findings for three dimensional simulations in Tregillis et al. (2001) and for cylindrical symmetry in Jones et al. (1999). The most important results have to do with the highly unsteady character of the flows. Those behaviors are illustrated in Fig. 1 for the currently reported simulation. The three panels are volume renderings of the bulk flow speed, the distribution of shocks and the distribution of magnetic field strength when the jet bow shock is almost to the end of the grid, so that the jet has propagated roughly 100 times its radius. We use a "color tracer" labeling plasma originating at the jet orifice to exclude material not associated with the jet and its backflow cocoon.

While the high speed jet flow clearly extends virtually to the nose of the cocoon, near its end the jet's motion becomes violently unsteady, so that it whips about and sometimes "breaks". This behavior is a response to the fact the the flows are highly driven, so naturally chaotic. Consequently there are actually only relatively brief moments when one can identify a classical, strong "termination shock" at the end of the jet. *Most of the plasma in the cocoon (and the high energy particles, most importantly) have escaped the jet without passing through a jet termination shock.* On the other hand the head of the cocoon itself is laced with shocks that form a kind of shock web. Those shocks process much of the backflow, and some of them are strong enough to be important CR acceleration. This leads to a much more complex pattern of CR spectra compared to the classical termination shock cartoon.

In addition, the whipping motion of the jet excavates an enlarged volume in the head region, so that the cocoon has an almost cylindrical shape rather than the parabolic form sometimes assumed (e.g., Loken et al. (1992)).

The cocoon magnetic field is also very complex and highly filamentary. The filamentation is, of course, a natural behavior of magnetic fields, and means that the field is quite intermittent. That is, there are wide point-to-point variations in the field strength, and most of the volume is filled with fields significantly weaker than the average field strength. In these simulations the magnetic stresses are relatively small, so the field structures are mostly carried along with the plasma. On the other hand, in a comoving volume the strength of the field will vary by large factors over time as the embedded field lines are stretched, relaxed or reconnected. Thus, in simulations we have done where radiative cooling is active,

the local rate of cooling is very unsteady. Consequent to all these features, spectral "aging rates" are very hard to predict by any simple model. Those models are certainly suspect as estimates for dynamical source ages.

Observational tests of radio galaxy models depend generally on nonthermal emissions; on synchrotron and Compton emissions, in particular. We compute synthetic observations of our simulated objects as a new and powerful tool to understand how dynamics translates into emissions, and to improve our ability to interpret observations of real objects reliably. Fig. 2 illustrates two pairs of surface brightness images synthesized for the simulated object shown in Fig. 1. The right pair corresponds to the same time as shown in Fig. 1, while the left pair shows the object when it is about $\frac{3}{4}$ as old. The top image in each pair constitutes a "synthetic" 1.4 GHz synchrotron map of the object, seen from a perspective similar to that in Fig. 1. The corresponding lower images show 10 keV nonthermal X-rays upscattered from the cosmic microwave background by roughly 1 Gev electrons.

There are obvious similarities and differences between the two kinds of emissions. In both, the jet is clear as it threads through the cocoon. It is especially bright in this electron model, since all CR electrons pass through the jet before being dispersed into the cocoon. On the other hand, while the cocoon itself has a similar general appearance in both bands, the details are substantially different. Although the two bands represent emissions from electrons of roughly comparable energies, the contributions are weighted very differently. The X-ray surface brightness is directly proportional to the column density of GeV electrons, so it shows explicitly where those electrons are most concentrated. The radio surface brightness, on the other hand, weights the electron column density roughly by the magnetic pressure. That, of course, is why the ratio of nonthermal X-ray to radio emission has the potential to provide meaningful measures of magnetic field strength in these objects. In detail the relative weighting factor depends on the electron spectrum. Particularly when radiative cooling steepens the spectrum on the high energy end that can be very important. For the simulation shown here, it is not very important, however.

Luminous radio galaxies typically display bright "hotspots" near the nose of the diffuse lobes. They are commonly identified as the jet termination shock. A strong termination shock in the simulated jet can produce a hotspot, as well. However, as mentioned, that dynamical feature is relatively uncommon in the simulated flows. Still, "hotspots" are generally visible in our objects. Several features resembling hotspots to some degree are present in Fig. 2, even though there is no termination shock at either time shown. This illustrates our finding that a number of situations can lead to hotspots, such as shocks in the web outside the jet, including those produced by jet "pieces" after separation. In that respect we find that apparent "guilt by association" with the jet can be misleading, since sometimes hotspots formed within the cocoon can be superposed onto the jet. All this serves to remind us that the flows are unsteady and complex.

5 Conclusions

We have applied novel numerical techniques to study the acceleration and transport of relativistic electrons in complex supersonic flows such as radio galaxies. We follow the base magnetized plasma with a conventional three-dimensional MHD code. The relativistic CR electron population is evolved using a simplified diffusion-advection equation integrated over finite momentum bins to reduce the computational costs to manageable levels. In the present simulations they represent about 50% of the effort.

With these methods we can study in some detail the relationships between flow dynamics and the properties of the CRs, including utilizing synthetic observations of the simulated objects based on self-consistent treatments of the nonthermal emissions. Radio galaxies have been modeled as derived from hypersonic light jet flows. We intend to explore a wide range of problems with these techniques, and have also adapted them to SNRs (Jun & Jones, 1999) and clusters of galaxies (Miniati et al., 2001a,b).

The most significant results associated with radio galaxies so far come from the impressive complexity that results from the highly driven nature of the flows. The ends of the jets develop into whips that stir up the cocoon of plasma that envelop it. That makes a strong termination shock uncommon, but creates a complex web of shocks laced through the head of the plasma that forms the radio galaxy lobes. Magnetic fields are highly intermittent throughout this structure. As a result the CR electron spectra have complex acceleration histories, and radiative losses are similarly difficult to characterize in any simple manner. We find that hot spots in the predicted emissions can result from a variety of physical behaviors, associated with flows the shock web, as well as with the jet terminus. Individual hot spots tend to be ephemeral.

Acknowledgements. This work is supported by NASA, NSF, KRF and the University of Minnesota Supercomputing Institute.

References

Clarke, D. A. in ASP Conf. Ser. 100., "Energy Transport in Radio Galaxies and Quasars", ed. P. E. Hardee, A. H. Bridle & J. A. Zensus (San Francisco: ASP), p311.

Heavens, A. F. & Meisenheimer, K., MNRAS, 225, 335–353, 1987.

Jones, T. W., Ryu, D. & Engel, A., Astrophysical Journal, 512, 105–124, 1999.

Jun, B.-I. & Jones, T. W., Astrophysical Journal, 511, 774–791, 1999.

Loken, C., Burns, J. O., Clarke, D. A. & Norman, M. L., Astrophysical Journal, 392, 54–64, 1992.

Miniati, F., Jones, T. W., Kang, H. & Ryu, D., Astrophysical Journal (in press), 2001.

Miniati, F., Ryu, D., Kang, H. & Jones, T. W., Astrophysical Journal (in press), 2001.

Ryu, D., Miniati, F., Jones, T. W. & Frank, A., Astrophysical Journal, 509, 244-255, 1998.

Tregillis, I. L., Jones, T. W. & Ryu, D., Astrophysical Journal, (in press), 2001.

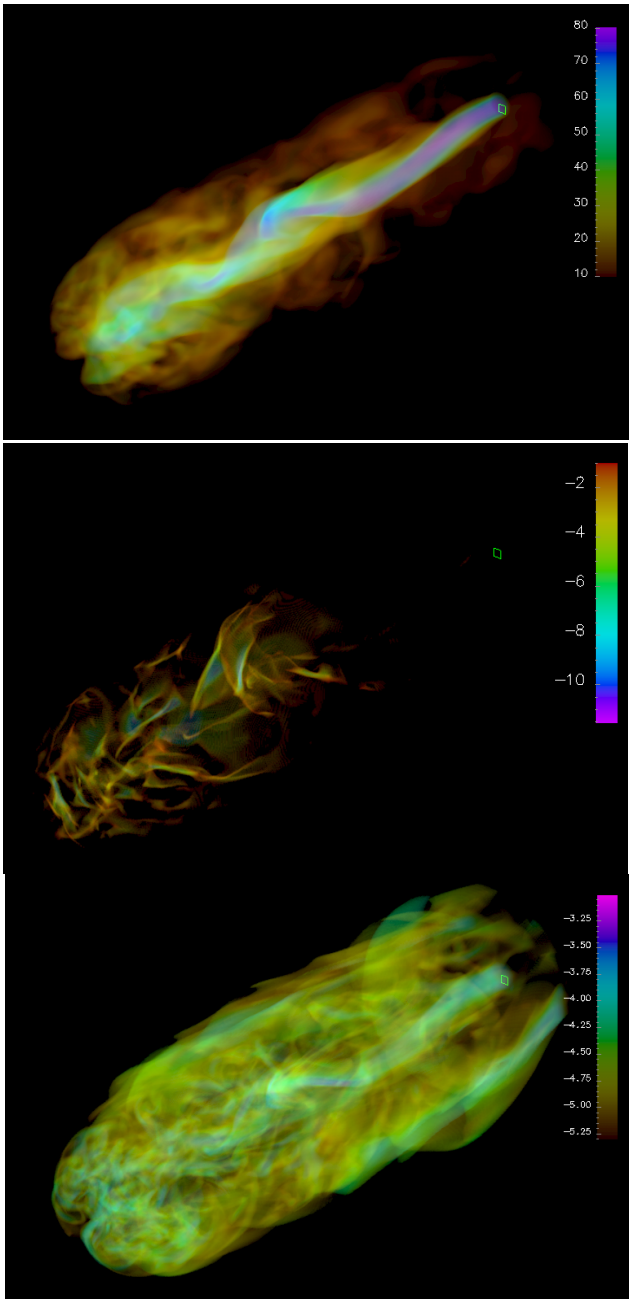

Fig. 1. Volume renderings of a simulated light Mach 8 MHD jet after it has propagated about 100 jet radii from its origin, shown by the square on the right in each panel. Shown top to bottom are: bulk flow speed, plasma compression ($\nabla \cdot u$) to locate shocks, and log of magnetic pressure. Right panels show the same time as Fig. 1; left panels when the jet has covered about $\frac{3}{4}$ that length.

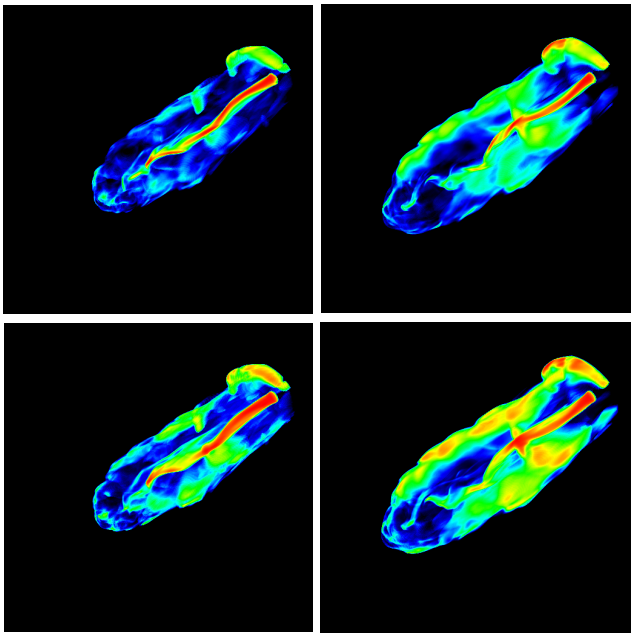

Fig. 2. Radio synchrotron (top) and X-ray CMB inverse-Compton (bottom) surface brightness images of the simulated flow shown in Fig. 1. The radio map corresponds to 1.4 GHz, while the X-ray map to 10 keV. Emissions are computed self-consistently, as described in the text. Each image is a logarithmic display; red corresponds to the highest intensity.